# How Many Reindeer? UAV Surveys as an Alternative to Helicopter or Ground Surveys for Estimating Population Abundance in Open Landscapes

**Paulsen Ingrid Marie Garfelt [1,a,b], Pedersen Åshild Ønvik [1,b], Hann Richard [2], Blanchet Marie-Anne [1], Eischeid Isabell [1,3], Van Hazendonk Charlotte[4], Ravolainen Virve Tuulia [1], Stien Audun [3] and Le Moullec Mathilde [2]**

[1]  Fram Centre, Norwegian Polar Institute, 9296 Tromsø, Norway
[2]  Norwegian University of Science and Technology, 7491 Trondheim, Norway
[3]  Department of Arctic and Marine Biology, UiT – Arctic University of Norway, 9037 Tromsø, Norway
[4]  The University Centre in Svalbard (UNIS), 9170 Longyearbyen, Svalbard

[a] Correspondence: ingrid.paulsen@npolar.no; Tel.: +47 96 91 36 86
[b] Ingrid M. G. Paulsen and Åshild Ø. Pedersen contributed equally to this work.

**Abstract:** Conservation of wildlife depends on precise and unbiased knowledge on the abundance and distribution of species. A challenge is to choose appropriate methods to obtain a sufficiently high detectability and spatial coverage matching the species characteristics and spatiotemporal use of the landscape. In remote areas, such as in the Arctic, monitoring efforts are often resource demanding and there is a need for cheap and precise alternative methods. Here, we compare an UAV pilot-survey to traditional population abundance surveys from ground and helicopter of the non-gregarious Svalbard reindeer to investigate whether small quadcopter UAVs can be an efficient alternative technology. We find that estimates of reindeer abundances from UAV imagery have lower precision and are more time consuming than present abundance surveys when used at management relevant spatial scales. We suggest that more efficient long-range fixed-wing UAVs should be evaluated for the job to increase the sampled area by UAV. In addition, the method will depend on the availability of more efficient post-processing methods including automatic animal object identification with machine learning and analytical methods that account for uncertainties.

**Keywords:** Aaerial survey; animal detection; distance sampling; helicopter; monitoring; strip transect; Svalbard; total count; ungulate

## 1. Introduction

The distribution and abundance of species are key statistics needed to estimate population trends, sustainable harvest strategies and in environmental impact studies [1]. Yet, it remains challenging to estimate population size with high precision and low bias at spatial scales relevant to management [2,3]. Numerous methods to estimate wildlife abundance and density exist ranging from direct population counts to population indices proportional to the true population size [4,5]. Abundant and easily detectable species are commonly monitored with direct density estimation methods, which includes complete or partial census, strip transect, distance sampling and capture-recapture programs [5,6]. Recent developments in UAV technology open new opportunities to survey animal populations as a replacement or supplement to traditional count methods [7]. UAV offers several advantages compared to traditional aerial or ground surveys [e.g., cost effectiveness, safety and operational range; 8,9], however, whether UAV methods have improved accuracy and are more efficient than traditional survey methods are largely unknown [but see 10,11].

Wildlife populations are traditionally counted by foot or using aerial surveys from helicopters or planes depending on the species characteristics and area of interest [e.g. 12,13-15]. Aerial surveys are costly, with a high carbon footprint and are challenging when

it comes to detectability and uncertainty estimates [16-19]. Counting on foot along a survey line is time-consuming and can be logistically difficult in remote areas or depending on the species [20]. In the last decade, uncrewed aerial vehicles (UAVs), remotely piloted aerial vehicles (RPAS), or drones – have been tested and successfully applied as a cost-effective alternative to traditional surveys to estimate abundance of wildlife, especially gregarious species [21,22], but also animals that are solitary [9,23].

Distance sampling and total counts are common methods that can assess precision and uncertainty in abundance surveys [4,24]. The former counts subsamples within a population and the latter the entire population in an area of interest. Both can be used to make density spatial models to predict densities across larger areas. A key assumption in distance sampling is that the probability of detecting an animal decrease with increasing distance from the observer. The advantage is that this can be used to include a measure of detection probability in the abundance estimation. Total counts assume that all animals within a certain area are detected [5], but can still include measures of detection error [20]. Total counts is often considered a more precise and less biased method than distance sampling and can be used as a reference population size [20]. For an aerial image survey (i.e., from crewed aircraft or UAV flying at constant height), detection is independent from distance from the transect line. Yet, there are other errors that can influence detection such as tree cover [17], landscape heterogeneity and image quality that should be accounted for in abundance estimates [15]. Integrating measures of detection error within a survey method and identifying habitat variables strongly correlated with the population of interest can greatly improve the accuracy of density estimates [3].

Ungulate populations are distributed in varying densities over large geographic areas and often with distinct seasonal habitat and range use [25], making precise counts logistically challenging and cost demanding. Therefore, the counts are often substituted with different type of indices [moose seen per hunter; 26,camera trap and dung; 27,28]. However, only recently UAVs are applied in surveys of ungulates, where restricted flight range relative to the spatial scale of interest for management and difficulties detecting and identifying deer, have been major obstacles [3,8,29-33].

In the High Arctic remote Svalbard archipelago, the wild Svalbard reindeer *Rangifer tarandus platyrhynchus,* is the largest resident mammalian herbivore in the terrestrial tundra ecosystem [34]. The reindeer is subject to long-term monitoring because it is a key-species impacting tundra vegetation [35], is harvested locally by recreational hunting [36] and is sensitive to climate change [e.g., 37,38]. The long-term monitoring is relying on total population counts along fixed routes on foot [20,39] or by helicopter [40], and capture-mark-recapture techniques [see 41 for a description of methods]. Lately, there has been focus on quality assurance and standardization of monitoring methods of the long-term total counts with distance sampling methods [20]. This has enabled range-wide monitoring of Svalbard reindeer using the most appropriate methodology according to terrain characteristics [42]. In addition there is a push for development of monitoring methods that reduces disturbance and lowers human footprints [43], which suggest the use of UAVs [44,45].

In this paper we compare counts from UAV imagery to counts from ground and helicopter of the Svalbard reindeer in a remote High Arctic tundra landscape. We test the feasibility of collecting data on reindeer abundance using UAVs and investigate potential problems and pitfalls associated with aerial monitoring as compared to ground-based surveys. Moreover, we assess the accuracy of UAV imagery to the traditional ground-based line transect distance sampling and helicopter surveys.

## 2. Materials and Methods

*Study area*

The Arctic Svalbard archipelago (74–81°N, 15–30°E)., Norway, is approximately 62,700 km² with approximately 60% covered by glaciers, 25% by barren rocks and only 15% by vegetation [46]. We conducted the study in Sassendalen, one of the largest valleys in Central Spitsbergen (Figure 1). The valley is surrounded by peaks up to 1200 m.a.s.l. and dominated by a large river and continuous vegetation cover with wetland, ridge, and heath present only in the valley bottoms and on the lower parts of the mountain slopes (<250 m.a.s.l.) [46-48].
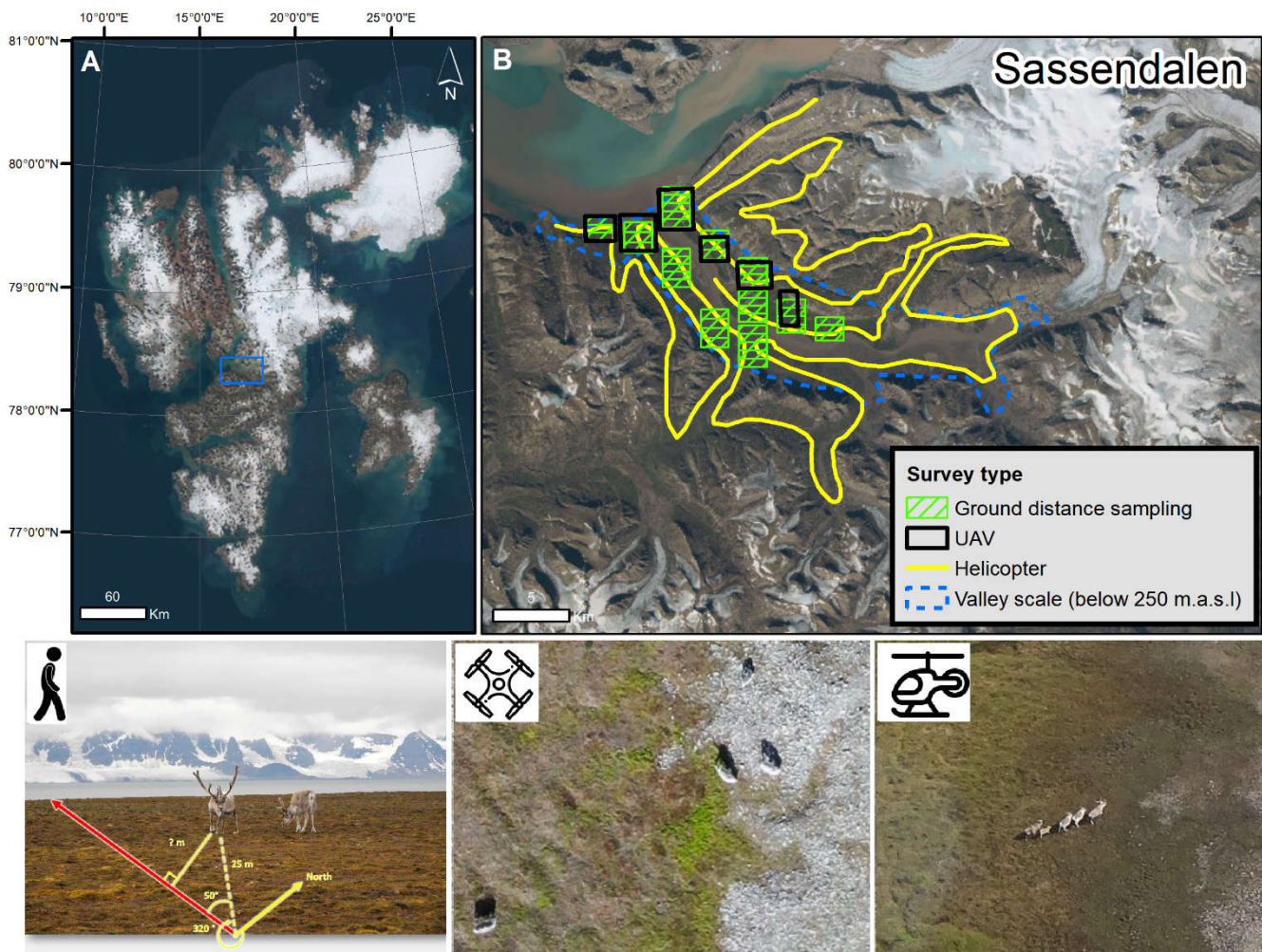
**Figure 1.** Upper panel: A) Svalbard archipelago. B) Overview of spatial data coverage for the three survey methods; ground DS (green), UAV (black) and helicopter (yellow) in Sassendalen, Svalbard. Lower panel: Raw images of Svalbard reindeer from the three types of survey methods. Left to right: ground distance sampling, UAV imagery at 120 m and helicopter (photograph from side window where one observer is sitting).

*Study species*

The Svalbard reindeer is distributed across all non-glaciated land areas of the archipelago, with an overall abundance of ~ 22 000 individuals and densities up to 10 reindeer/km² [42]. Svalbard reindeer are mostly solitary and virtually free from predation, although rare attacks by polar bears (*Ursus maritimus*) have been observed [49,50]. Direct density dependence and large annual variations in weather conditions — notably the amount of rain in winter, but also the length of the snow-free season in the autumn — shape the reindeer's body condition and vital rates [37,41,51,52]. This, in turn, causes large annual fluctuations in population abundances [41,53].

*Field data collection*

For the UAV survey and ground-based distance sampling surveys (hereafter ground DS), we allocated 10 transect lines in north-south direction, from the mountain foothills to the riverbanks, on each side of the main river in Sassendalen, Svalbard (Figure 1B). We chose one random latitude for the first line and placed additional parallel transect lines systematically apart 2.5 km east or west from this latitude to avoid overlapping reindeer observations and violation of the assumption of independence for DS surveys [24]. We chose this systematic orientation across the valley (i.e., river bed to mountain side or vice-versa) to reduce any bias from potential gradients in animal density related to e.g., plant phenology and/or habitat configuration [54]. The strip length of each of the transects varied depending on the length from the mountain side to the riverbank (1.2 km to 2.9 km). The UAV and DS surveys were conducted within the same three-day period 14-17 July 2021, but with a time interval (1 day) between methodologies to allow the free distribution of reindeer in case of disturbance by observers. The helicopter survey was conducted one week prior to the UAV and DS surveys (6 July) and was part of an annual census of reindeer in the valleys on Nordenskiöld Land by the Governor of Svalbard (Figure 1B). See Figure 2 for an illustration of the workflow.
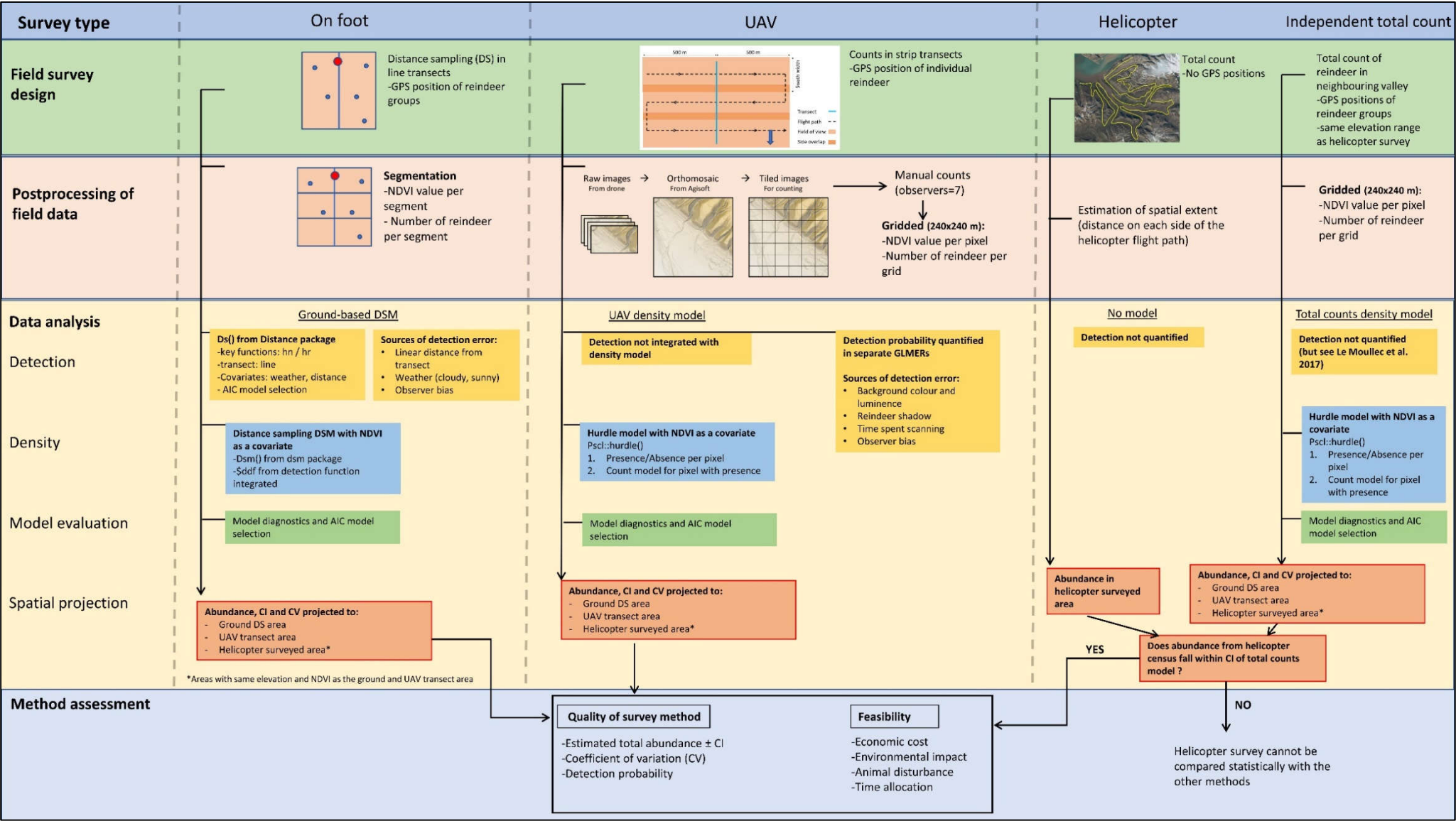
**Figure 2**. Visualization of the workflow, including field survey design, postprocessing and data analysis.

Ground distance sampling survey

We followed the DS survey protocols described by [20,42] for estimating abundance of Svalbard reindeer. The 10 transects were walked by one observer at a constant speed (2–3 km h$^{-1}$) without stops, except during measurements. We used a handheld GPS and a compass to keep the line direction, and single reindeer or clusters were detected on both sides of the transect line with the naked eye. To respect the assumption of constant detection along the transect line, no scanning of the surroundings was done when stopping to take measurements. Each observation was measured by laser binoculars (10×42 Leica Geovid) to the nearest meter and a compass was used to measure the angle from the observer to the reindeer (Figure 1). Note that this method does not record the population structure (i.e., age and sex). The geographic position of the observer was also recorded. For practical reasons when using the laser, measurements were taken to the largest reindeer (e.g., a mother rather than her calf) or the middle individual of a group of adults. From the DS survey, the GPS positions of reindeer groups was calculated and used in the final dataset.

UAV survey

Six out of the ten line transects were mapped by an off-the-shelf DJI Mavic 2 Enterprise drone, equipped with a zoomable (24–48mm) RGB camera. Flight plans for each line transect were prepared pre-flight with a commercial mapping software (DJIFlightPlanner). The flight plans were flown automatically with flight altitude 110–120 m above ground with a nadir (downward-looking) orientation of the camera. Test flights with different altitudes were performed before the survey to verify that reindeer could be detected on images at that height and to ensure that reindeer were minimally disturbed. At this altitude, the widest field of view (i.e., 24 mm) was used, giving a theoretical ground sample distance (GSD) of 4.4 cm and a swath width of 174 m. Side overlap was chosen with 65% and the nominal forward overlap with 85%. All lines had a run separation of 61 m and ran in an east-west direction. Ground speed was set to maximum 30 km/h and pictures taken with a frame rate of 2 s. The camera settings were on auto, but it was ensured that the shutter speed would not exceed 1/200 to prevent motion blur (max. shutter speed = GSD/ ground speed), else flight velocity was reduced. The total mapped area width covered 500 m on each side of the transect line. The total length of the mapping flight lines was between 20–40 km and typically took between 2–4 batteries to cover.

Helicopter survey

Reindeer were counted by four observers (two pilots and two observers) in a Super Puma helicopter flying 60–100 metres above the ground according to protocols by the Governor of Svalbard. This census has been done annually since 1998 by the Governor of Svalbard as background information to determine the annual hunting quota of reindeer [40,55]. The flight path (Figure 1), were assumed to cover the most important reindeer summer habitats in the Sassendalen hunting unit (see Peeters, *et al.* [56] for a map of hunting units). The census provides a single total count of all the individuals encountered, classified as calf, female/young and male, without any information on location of each animal.

*Spatial covariates*

Le Moullec, Pedersen, Stien, Rosvold and Hansen [42] found that the best environmental predictor for reindeer densities in summer is vegetation productivity at the peak of the growing season, measured by maximum normalized difference vegetation index (maxNDVI). Since cloud coverage affects the maxNDVI at pixel level and can contribute to random variation in the timing of maxNDVI, we chose to use a five-years (2017-2021) average maxNDVI rather than single year maxNDVI [57,58]. NDVI was collected from the MODIS-satellites and resampled to 240×240 m.

*Data analyses*

To compare the three survey methods (ground DS, UAV, and helicopter) of Svalbard reindeer we developed density spatial models (DSM, Figure 2). The statistical models were adapted from Le Moullec et al. (2017, 2019). Details on each step of the data analysis are outlined below. We fitted all models in R version 1.4.1717 [59].

Ground distance sampling survey

The ground DSM consisted of a two-stage approach with a detection probability estimation and a density spatial model accounting for the imperfect detection [24]. To prepare the data, we divided the transect lines into smaller segments to summarise count data and maxNDVI, as recommended by Miller et al. (2013). We divided the transects into equal lengths of 500 m (for effect of segment lengths on model output, see Table S1 in Le Moullec, Pedersen, Stien, Rosvold and Hansen [42]) and truncated the transect width to 95 % of all distances rounding up to the nearest reindeer group.

We modelled detection probability using half-normal and hazard-rate functions and determined the top ranked model using AIC. We included weather (sunny or cloudy) as a covariate since weather was the main covariate influencing detection in Le Moullec, Pedersen, Stien, Rosvold and Hansen [42]. The hazard rate function with weather as a covariate had the lowest AIC and was thus selected for the density function (Appendix A). We used the most parsimonious density model from Le Moullec, Pedersen, Stien, Rosvold and Hansen [42], which modelled individuals per segment as a function of maxNDVI using a log-link quasi-Poisson model. The final model was fitted using the restricted maximum likelihood (REML) framework and residuals were checked for normality, auto-correlation, and goodness of fit (Table A2, Figure A2). We used the standard distance sampling functions 'ds', 'dsm' in the packages *Distance* and *dsm*, respectively.

UAV survey

The UAV survey generated a larger number of single images (n=10,479) with considerable image overlap. To reduce the number of images to be reviewed for counting of reindeer, the single images were processed into orthomosaic images for each transect line using a structure from motion method in Agisoft Metashape. The orthomosaic images were typically large (ca. 30,000×40,000 pixels covering areas between 1.5–3.4 km², GSD between 3.7–4.1 cm/pixel) and were segmented into smaller tiles of 4,000×3000 pixels with a 10% overlap to ensure that animals on the border of the tiles could be identified. Observers (n=7) manually counted reindeer on each tile (see protocol in Appendix B). Positions and image

snapshots of detected reindeer were stored for each observer. In addition, all single images were counted by 3 observers to check if reindeer were lost or appeared twice in the processing steps or due to reindeer movement. This resulted in the detection of four reindeer that showed up more than once and these copies were excluded. Further, all detected reindeer were scanned a third time and assigned a certainty category ('low', 'medium', and 'high') according to how clearly a reindeer (and not a rock or similar grey structure) was visible on the image snapshot. Only reindeer that were assigned to certainty category 'medium' or 'high' were used in the final dataset. We termed this dataset 'confirmed' reindeer. Furthermore, we divided the area of the six UAV transects into grids with the same resolution as the resampled maxNDVI layer (240×240 m) and summarized the number of confirmed reindeer per pixel.

Since reindeer detection was imperfect among observers, we further investigated what caused this variation. We tested if background color (i.e., grey colored reindeer on green background would stand out more than on grey backgrounds) or luminance (lower detection of reindeer on darker images) influenced observer detection at the image unit. We extracted median luminance and mean RGB values from each tiled image, and from the mean G and B values we calculated a greenness index [G--B; 61]. The covariates were tested in separate linear mixed effect models due to multicollinearity with the 'glmer' function in the *lme4* package to investigate the probability that 1) an observer detects a reindeer on an image (presence/absence model, Appendix C) and 2) when they do, how many reindeer are detected on that image (counts model, Appendix C).

Based on the dataset with 'confirmed' reindeer counts, we fitted a hurdle model to avoid overdispersion from the high number of pixels with no reindeer observations. The hurdle model deals with the response variable in two stages, 1) the presence-absence of reindeer in a certain unit (i.e., pixel) and 2) a count model estimating how many reindeer were present in that unit (when reindeer were present). The final hurdle model contained a zero-truncated negative binomial distribution with a dispersion parameter, where maxNDVI was used as a covariate assuming a logit-link function in both the presence-absence and the count model (Appendix D). This was done with the function 'hurdle' in the package *pscl.* The residuals for this model were checked for normality, autocorrelation, and goodness of fit.

Helicopter survey

The helicopter survey covered a larger extent and wider ranges of terrain features and vegetation classes (see Figure 1) than the ground DS and UAV surveys. The helicopter survey lacked positional information on individual reindeer or groups and no distances to calculate detection probabilities, which was a major obstacle for comparison with the other survey methods. To overcome this fact, we took advantage of another quality assured total counts dataset in an adjacent area (Adventdalen, Appendix E) for abundance calculations. Reindeer densities in the main valleys in Nordenskiöld Land are strongly synchronized with each other due to winter weather effects and summer warming leading to spatially autocorrelated survival and mortality [37]. This led us to anticipate similar population densities between the adjacent valleys. Given that reindeer densities are strongly positively correlated with maxNDVI and total counts can be used as a reference population model [20,42] we projected the total counts model across the helicopter surveyed area in Sassendalen

as a function of maxNDVI to give us similar values (i.e., within the confidence interval) as the actual abundance from the helicopter census in Sassendalen. We first modeled the number of reindeer per pixel in the helicopter surveyed area as a function of maxNDVI using total counts from the Adventdalen census (hereafter termed 'independent' total counts) that covered the same range of terrain features and vegetation classes. To derive the spatial extent of the helicopter surveyed area, the entire flats of Sassendalen and a buffer of 1 km (500 m on either side of the helicopter) around the transect line in the mountains were included. The best model from the total counts model selection process in Le Moullec *et al*. [42] was used on the dataset and model diagnostics were assessed. Details on the procedure are outlined in Appendix E.

*Comparison of survey methods*

To assess each survey method, we compared their DSM as a function of vegetation productivity (maxNDVI) and then predicted each model across 1) the ground DS covered area 2) the UAV covered area, and 3) at an ecologically relevant valley scale that also shared similar vegetation productivity and elevation range between the three survey methods (Table S1). Since the elevation range was higher for the helicopter surveyed area (0.6-601 m) than for the ground and UAV transect area (0.7-317 m), we did not predict the ground DS and UAV density models to the helicopter surveyed area. Precision of the methods was assessed by comparing confidence intervals within the sampling areas (i.e., smaller width of confidence intervals indicates lower sampling error) and coefficient of variation (CV), which is the ratio of the standard deviation to the mean (i.e., lower CV indicates higher precision). In addition, we qualitatively evaluated the methods according to their feasibility i.e., time allocation, economic cost, environmental impact, and wildlife disturbance.

## 3. Results

*Field survey characteristics*

The ground DS survey detected 50 groups of reindeer (n=104 individuals, mean group size = 2) from walking 23.6 kilometers on foot with a transect truncation width of 907 m (i.e., covering an area of 42.7 km², Figure 1). The UAV survey, which covered about half of the same transects (23.5 km²), detected 32 confirmed reindeer. The helicopter survey covered the largest area (286.2 km²) and resulted in 1559 observed reindeer. Thereby, the UAV survey gave lower reindeer density (1.4 reindeer/km²) than the ground DS survey (2.4 reindeer/km²) and the helicopter survey (5.4 reindeer/km²). The range in vegetation productivity between the sampling areas were similar for all methods, with a mean maxNDVI around 0.50 (range: 0.78 [DS], 0.75 [UAV] and 0.81 [helicopter], respectively).

*Detection*

The average detection probability for the ground DS was $0.40 \pm 0.10$ (CV = 0.24) and 30% of the reindeer clusters were detected at approximately 500 m. Sunny weather resulted in higher reindeer detectability than cloudy weather (Figure A1). For the UAV survey, the average detection rate of confirmed reindeer varied between 46-70% between observers (n=6). Variation of reindeer detection on the UAV imagery for the presence/absence model showed an association with the greenness index and

blue color channels when accounting for observer variability (Figure C1). High values in the greenness index increased detectability (intercept ± se = 3.56 ± 0.93, Figure C1), while blue channel decreased presence detectability (3.06 ± 1.48). In addition, all variables decreased the probability to counts the correct number of reindeer on an image when at least one reindeer was present (luminance -2.66 ± 0.57, greenness: -0.52 ± 0.22, red channel: -3.91 ± 0.76, green channel: -3.61 ± 0.72, blue channel: -2.24 ± 0.58) (Figure C2).

*Density spatial models*

All three DSMs predicted a positive correlation between vegetation productivity (maxNDVI) and reindeer densities (Figure 3). Reindeer density remained low until around maxNDVI of 0.6-0.7 and thereafter increased steeply. However, the strength of the relationship was markedly lower for UAV, while the ground DSM and total counts were similar (Figure 4).
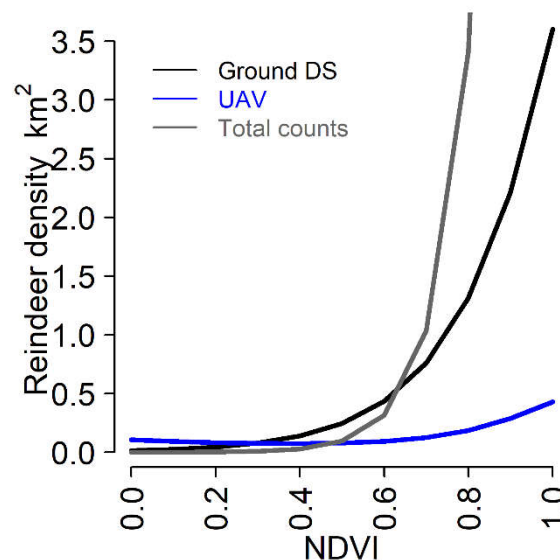
**Figure 3.** Predicted density of Svalbard reindeer (number of animals per km²) based on data from the three different survey methods (ground DS, drone, and independent total counts) and maxNDVI (i.e., proxy of biomass production). Hurdle models applied to the drone and helicopter survey data and the lines show predicted density based on the total count density model for Adventdalen (neighbouring valley) and the drone imagery at valley scale.
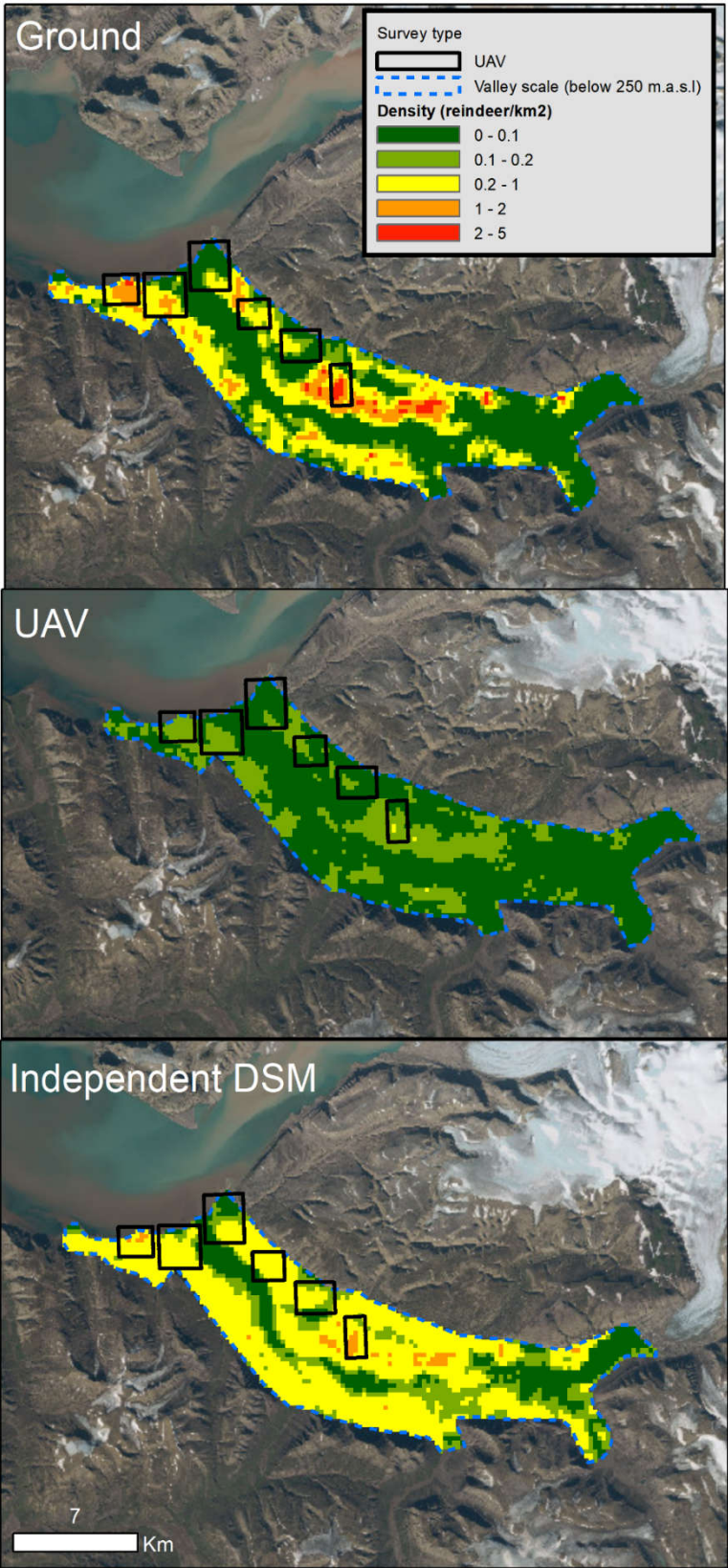
**Figure 4.** Predicted density (number of animals per km²) of Svalbard reindeer based on density spatial models with maxNDVI as a covariate for the ground line transect distance sampling (upper), UAV survey (middle) and independent total counts model from a neighboring valley at the valley scale. The map shows predicted densities at the valley scale for pixel resolution of 240 × 240 m.

*Spatial projections*

The independent total counts model from the neighboring valley estimated similar abundances in the helicopter surveyed area (1515 ± 67, CV = 0.06) as the helicopter survey (n=1559) (Table 1). For both the ground DS and UAV sampling areas, the UAV density model estimated the lowest abundances but also had the smallest confidence interval, while the ground DSM and total counts DSM estimated more similar abundances. The independent total counts DSM had the lowest CV. For the valley scale, the ground DSM and total counts DSM fell within each other's confidence intervals, while the UAV density model grossly underestimated the abundances (Table 1). Thus, the UAV density model had the highest sampling error, and the ground DSM and independent total counts DSM had the lowest coefficient of variation. The UAV were imprecise and strongly underestimated abundance at all spatial scales compared to the other methodologies having matching estimates.

**Table 1.** Estimated Svalbard reindeer abundance ± confidence intervals (95%) in Sassendalen from density spatial models (DSM). Predicted abundance for each density model at three scales; Ground DS scale (area covered on foot), UAV scale (area covered by UAV), and valley scale. See Figure 1 for delineation of study areas. The total counts DSM is based on total count from a reindeer population in a neighboring valley. Coefficient of variation in parentheses. Since the elevation range was higher for the helicopter surveyed area (0.6-601 m) than for the ground and UAV transect area (0.7-317 m), we did not predict the ground DS and UAV density models to the helicopter surveyed area.

| Survey method | Estimated abundance | | | |
|---|---|---|---|---|
| | Ground DS sampling area | UAV sampling area | Helicopter surveyed area | Valley scale |
| Ground DS | 125 ± 66 (0.27) | 185 ± 125 (0.25) | - | 919 ± 588 (0.22) |
| UAV | 72 ± 62 (0.47) | 40 ± 100 (0.81) | - | 256 ± 141 (0.28) |
| Helicopter | - | - | 1559* | - |
| Independent total counts | 311 ± 94 (0.14) | 161 ± 68 (0.19) | 1515 ± 67 (0.06) | 958 ± 160 (0.08) |

*Actual abundance estimate from helicopter survey

*Feasibility*

The feasibility of the survey method varied widely (Table 2). In terms of field time, the helicopter census covered by far the most ground in the least time (1 hour), while the ground DS (10 hours) and UAV survey (12 hours) was much slower. In terms of data processing time, the UAV images took the most time due to large amount if imagery. However, the helicopter survey had the highest expenses, environmental carbon footprint and disturbance and did not record geographic positions.

**Table 2.** Feasibility of the three survey methods in terms of spatial extent, time allocation, economic cost, environmental impact (carbon footprint) and animal disturbance.

| Survey method | Spatial extent | Time allocation | Economic cost | Environmental impact | Animal disturbance |
|---|---|---|---|---|---|
| Ground DS | Medium (42.7 km²) | Field time: 10 h<br>Processing time: medium | Low | Low | Medium |
| UAV | Low (23.5 km²) | Field time: 12 h<br>Processing time: high | Medium | Low | Low |
| Helicopter | High (286.2 km²) | Field time: 1 h<br>Processing time: low | High | High | High |

## 4. Discussion

Our comparison of three different survey methods — ground DS, UAV, and helicopter surveys — for estimating Svalbard reindeer abundance and density showed that abundances derived from UAV imagery had lower precision and were more time consuming due to processing time than ground DS and helicopter surveys. However, from the UAV survey it was possible to correctly identified reindeer, calculate precision and factors affecting observer detection to compare with other methods. The scale of precision is still at a reasonable level in the UAV survey and can be improved in the future by addressing some key challenges.

Imprecise estimation of abundance can result from a variety of sources, including violation of major statistical assumptions, survey design and observer variability [3]. Here, the estimated abundances based on UAV imagery, gave lower and more imprecise abundance estimates than total counts or ground distance line transect sampling. This is likely attributed to the low spatial extent of the UAV area, which was approximately half of the ground DS sampling area. Doing repeat surveys over the same transect lines may increase accuracy [30]. The helicopter survey had a higher density (5.4 reindeer / km²) than the UAV survey and ground DS survey (1.4-2.4 reindeer / km²). The helicopter survey covered more area per time unit than the ground DS and UAV survey, but lacked systematic survey design and estimates of uncertainty, which made it challenging to compare and increased the risk of double counting reindeer. By comparing with an independent total counts model from a neighbouring valley, we were able to assess how reasonable the abundance from the helicopter survey was. Total counts are viewed as less biased and more precise compared to distance sampling and can be used as a reference population [20], which was also the case in this study. For the helicopter survey, a larger sample size (i.e., more transect lines and a larger number of observations), records of reindeer geographic positions and assessment of detection would increase the quality of measurements and allow for a more thorough investigation of the at the larger valley scale.

We assessed detection probability for the ground DS and UAV survey. For our UAV survey, we evaluated whether detection was impacted by landscape texture, such as colour on the background of the UAV imagery (i.e., a reindeer would stand more out on a green, vegetated background than on a grey, gravely background). We found that the greenness index and the blue values influences observer ability to detect if there was a reindeer present. Blue as a dominant reflection can be due to non-vegetated areas (e.g., gravel). In the counts model, all covariates influenced observer detection, but this is likely due to the low number of images with

more than one reindeer. Unfortunately, we were not able to find any available functions in R packages integrating detection probability in a density function for drone imagery (i.e., where detection is independent of distance to sampling area, but where covariates exist). For instance, the strip transect framework, modelled with a uniform key detection function (in 'ds' in *Distance* package) or both model parts of a hurdle model (presence/absence and count model in hurdle() in *pscl* package) does currently not allow adding covariates in the detection function. As the use of UAVs in wildlife studies increase, developing such analytical framework is highly needed for the integration of imperfect detection, as we demonstrate here.

The spatial distribution of reindeer relative to area covered also poses a challenge. Particularly, for the UAV imagery, the number of observations of individual reindeer or groups was limited. Reindeer in Svalbard typically occur solitary or in small groups opposed to most reindeer and caribou that appear in herds, and as such can easily remain unidentified on the images. In contrast, to more gregarious or colony species [21,22], the low density of reindeer challenged not only the sample size, but also detection of animals leading to large observer variability [19]. To overcome this, we suggest applying a drone with longer range to increase area covered and types of tundra habitats with different texture and number of observations of reindeer.

The UAV used in this pilot study is a small quadcopter drone, with limited battery capacity and flying time. Using larger quadcopter drones or fixed-wing drones with a longer range is suggested to allow for larger area covered over which abundance can be estimated [44,62]. This, however, comes at larger cost and – in the case of fixed-wing drones – higher operation complexity, particularly in the Arctic. Thus, it was a sensible approach to first verify the methodology with small quadcopters first. Once the method is fully evaluated and developed it can be easily transferred to more complex UAV systems that compensate for the limited range and coverage (i.e., using fixed-wing UAVs). Practically, such surveys should be conducted with fixed-wing UAVs that have longer range and can cover larger areas [44].

Here we conducted the survey in an open tundra landscape with good visibility from the air (at 120 m) and no terrain obstacles hindering the drone. This flying height permitted the maximum area to be covered at which a reindeer could be detected with minimal reindeer disturbance. Retrospectively, we could have increased detection of animals (i.e., observers would have been less uncertain to distinguish an animal from a rock) at a lower altitude and smaller ground sample distance. This would come at the cost of longer flight times due to lower swath width (i.e., denser mapping flight lines). A way to compensate for the increased flight time would be to reduce the side or forward overlap to a lower value. If no generation of terrain information (e.g., a digital elevation model) is required, overlap can be reduced below 50%, thus substantially decreasing the amount of flying time coarsening mapping flight lines. Before deciding to fly at a lower height, the effect of UAV disturbance on reindeer should be carefully assessed in a separate study. From our preliminary field investigations, the reindeer in Sassendalen was not visibly disturbed at 120 m, but different reindeer populations may act differently to a UAV, and some populations are shyer as they encounter humans less frequently [63].

The large number of images that our UAV survey produced exemplifies key challenges of any aerial survey method – counting the animals in the images. To increase the efficiency of the process, orthomosaics were generated and then tiled into "easy-to-handle" single images. This reduced the number of images to scan by an order of magnitude and made the process substantially more efficient. In the stitching process, reindeer may disappear or appear multiple times. By scanning and comparing the raw imagery with the tiled imagery after the stitching process, we quantified this disappearance, but at the expense of much longer processing time. In the case of the disappearing reindeer, the reindeer was moving over heterogenous terrain (from riverbed into swamp). This large gradient in background may explain why the algorithm resulted in removing the reindeer in the stitching process. However, reindeer that remained stationary, moved few meters, or moved over homogenous terrain did not appear multiple times nor disappeared in the orthomosaic process. Another challenge with the large number of images is related to observer variability. Scanning many images with multiple empty images can results in fatigue and decreased attention span. Datasets from UAV surveys with low-density populations in homogenous, open landscape seem particularly well-suited for automated counting methods, e.g., using machine learning [64] and developing a larger training dataset for reindeer detection would be key to towards automated detection methods. This study confirms that UAV technology can be an alternative method to traditional population monitoring methods of tundra herbivores, although more trials on UAV type relative to spatial coverage and advancements of pre-processing and machine learning is indeed needed to "speed up" efficient use of the technology in open remote tundra landscapes.

## 5. Conclusions

Reliable estimates of wildlife population abundance provide management with the information necessary to take conservation and management decisions. Our results show that UAV survey has the potential to be an alternative to traditional wildlife monitoring methods, as we could count and collect geographical positions of reindeer for estimating abundance, variance and quantify detection error from the UAV imagery. Some limitations that arises from small sampling area and long processing time in the UAV survey could be overcome by using a fixed-wing UAV to cover a larger spatial area and develop a training dataset that could be used for machine learning algorithms to automate the counting process. The relative lower carbon footprint and lesser human disturbance compared to helicopter surveys encourages further UAV method development in the Arctic in the years to come. Before the limitations are addressed, UAV will function as a supplement to the traditional "old fashion" field methods and cannot yet fully replace them for monitoring low-density herbivores in open landscapes. Our study demonstrates an example of the importance of a thorough quality assessment of survey methods before results are applied for management inference.

**Author Contributions:** Å. Ø. Pedersen and I. M. G. Paulsen have contributed equally the article. Conceptualization, Å. Ø. Pedersen, I. M. G. Paulsen, M. Le Moullec, Isabell Eischeid, Audun Stien and V. Ravolainen.; methodology, M. Le Moullec, I. M. G. Paulsen, M. A. Blanchet, Å. Ø. Pedersen and R. Hann; software, R. Hann and I. M. G. Paulsen; formal analysis, I. M. G. Paulsen, M. Le Moullec, M. A. Blanchet and R. Hann; investigation, R. Hann, M. Le Moullec, I. M. G. Paulsen, Å.Ø. Pedersen and C. M. van Hazendonk; resources (equipment, environmental

data etc.), R. Hann, I. G. Paulsen, Å. Ø. Pedersen, V. Ravolainen; writing—original draft preparation, Å. Ø. Pedersen, I. G. Paulsen, M. Le Moullec and R. Hann; writing—review and editing, all.; visualization, I. M. G. Paulsen and M. Le Moullec.; project administration, Å. Ø. Pedersen; funding acquisition, Å. Ø. Pedersen, I. M. G. Paulsen, M. Le Moullec, Audun Stien, and V. Ravolainen. All authors have read and agreed to the published version of the manuscript.

**Funding:** This research was funded by Svalbard Environmental Protection Fund, Svalbard Int grated Arctic Earth Observing System, the Norwegian Polar Institute and Norwegian University of Science and Technology.

**Data Availability Statement:** Hann, R. 2022. Drone-based mapping of Sassendalen for reindeer counting in Svalbard. DataverseNO. V1. Doi: 10.18710/KHQKWH

Pedersen, Å. Ø. (2022). Svalbard reindeer distance sampling dataset in Sassendalen 2021. Norwegian Polar Institute. Doi: 10.21334/npolar.2022.8f2c11ff

**Acknowledgments:** We thank Jørn Dybdahl for excellent support during the field work, Oddveig Øien Ørvoll and Bernt Bye for cartographic assistance and the Governor of Svalbard for use of the Fredheim cabin. We also thank the people that counted the reindeer imagery David Studer, Anna Caroline Grimsby, Beate Garfelt, and Stein Tore Pedersen and Stein Rune Karlsen for providing NDVI-maps.

**Conflicts of Interest:** The authors declare no conflict of interest.

**Appendix A: Model selection and detection curve for estimating Svalbard reindeer abundance by Distance Sampling**

**Table A1.** The 4 candidate detection probability models for distance sampling (DS) of Svalbard reindeer, Svalbard, Norway (July 2021). Detection probability was fitted using half-normal (hn) and hazard rate (hr) functions with weather (sunny or cloudy) as covariate (see Table S3 in Le Moullec *et al*. [42] for the influence of other covariates). We ranked models using Akaike's Information Criterion (AIC) and differences in AIC (Δ AIC).

| Model | Key | AIC | ΔAIC |
|---|---|---|---|
| ~ weather | hr | 657.893 | 0 |
| ~ 1 | hr | 661.477 | 3.584 |
| ~ weather | hn | 663.627 | 5.734 |
| ~ 1 | hn | 665.857 | 7.964 |
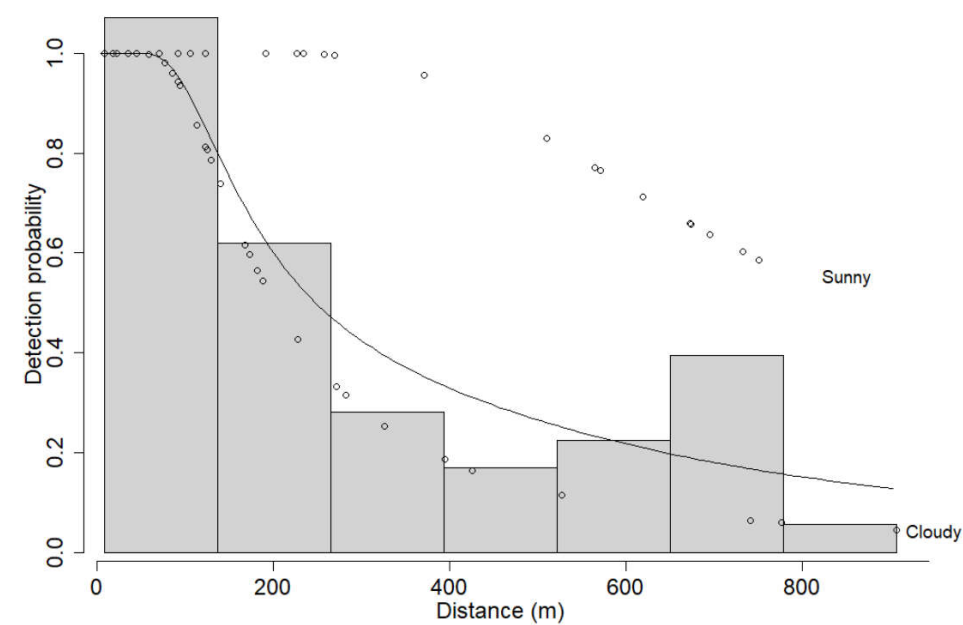
**Figure A1.** Detection probability function based on the line transect distance sampling of Svalbard reindeer. The best model was fitted at a continuous scale for observed distances and included a hazard rate key detection function with weather (sunny or cloudy) as covariate. Observations of reindeer clusters are illustrated by dots along the curve.

**Table A2.** Density model obtained from ground distance sampling. We used the most parsimonious density model from Le Moullec *et al.* [42], which modelled individuals per segment as a function of NDVI using a log-link quasi-Poisson model. This model was fitted using the restricted maximum likelihood (REML) framework.

| | **Ground DS survey Sassendalen** | | **Model by Le Moullec et al. (2019)** | |
|---|---|---|---|---|
| | $\beta \pm$ SE | *P* | $\beta \pm$ SE | *P* |
| Intercept | -19.25 ± 2.05 | <0.001 | −13.95 ± 0.38 | <0.001 |
| NDVI* | 0.012 ± 0.003 | <0.001 | $2.65 \times 10^{-3} \pm 0.76 \times 10^{-3}$ | <0.001 |

\* Le Moullec et al. 2019 is based on average max NDVI from 2013-2016.
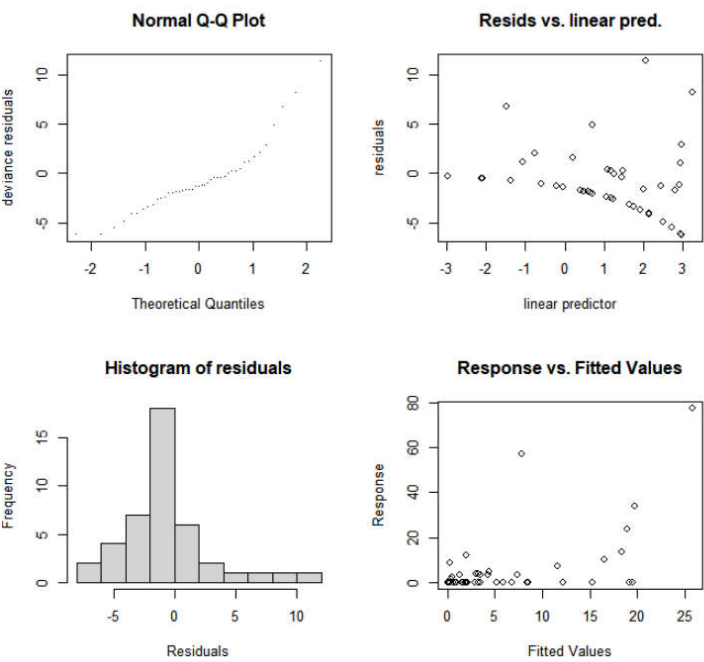
**Figure A2**. Density function modelling individuals per segment as a function of NDVI using a log-link quasi-Poisson model. The model was fitted using the restricted maximum likelihood (REML) framework. Displayed above are diagnostics for the selected model using the function 'gam.check' in the package *mgcv*.

**Appendix B: Protocol for counting reindeer from UAV imagery**

**Counting Svalbard reindeer from drone imagery - instructions to observers (full version can be available from the authors upon request)**

*Background*

In this protocol you will count Svalbard reindeer in UAV imageries captured in Sassendalen, Svalbard in July 2021. Six predefined transects were flown with a multirotor at an altitude of 100-120 meters above ground in reindeer habitat. The images where merged and postprocessed into evenly sized tiles by Richard Hann (NTNU). The objective for you as an observer is to help identify reindeer from the UAV imagery and assign them into simple sex and age categories to compare with helicopter and ground surveys done the same year.

The software you will use to count the reindeer is called DotDotGoose. DotDotGoose is a free, open-source tool to assist with manually counting objects in images. The software was created by the American Museum of Natural History to assist conservation researchers and practitioners working on counting objects in any kind of image format. The benefit of DotDotGoose is that you can easily create custom classes, pan and zoom on images and place points to identify individual objects. The metadata from each observer will be exported for further analyses in this project.

The reindeer categories you will identify in the UAV images correspond to sex and age classes used in helicopter counts (Governor of Svalbard 2009) and ground surveys [total counts; 20]. These are 1) reindeer with large antlers (old male), 2) reindeer with small antlers (female/young), 3) reindeer without antlers female/young, 4) calves 5) reindeer you are unsure which category it belongs to, and 6) carcasses. Carcasses are not counted from helicopter surveys but come in addition because it will help you to keep focused since there are many images without reindeer on them.

The categories may look like the photos below on the UAV imagery (Figure E1 and E2). Note that key characteristics of a reindeer is the body shape, colour (white and grey) and sometimes shadow. The shadow can sometimes help to determine the size of the antlers (if antlers are present). Be aware that the objects are pixelated and blurry and it may not always be easy to distinguish the objects, especially if reindeer are lying down.

| Reindeer with small antlers | Reindeer large antlers | Reindeer without antlers |
|---|---|---|
|

 |

 |

 |
| Reindeer with small antlers have less clearly defined antlers or the antlers are much smaller compared to their body size. | Reindeer with large antlers have a clear, protruding large v-or u-shape in one end, large compared to their body size. | Reindeer with no antlers do not have any clear protruding shape from their body. |

| Calf | Carcass |
|---|---|
|

 |

 |
| A calf is determined by the relative smaller size compared to the surrounding reindeer (the calves are always with another female reindeer at this time). | Carcasses may look like above with white hairs scattered around. Note, also the antlers next to it. |

Overview of the five classes to categorize reindeer into from the drone imagery.

A full-scale image like the one you will see when you go through the images and classify reindeer into one of the five categories in Figure E1. Do you see a reindeer? Try to remember the size of the reindeer relative to the full-scale image. If you see anything that resembles a reindeer you can zoom in using the buttons on the left.

For more information about the software (other than what is in this protocol) check out the DotDotGoose Quick-Guide in the folder or this video tutorial on how to use the software: https://www.youtube.com/watch?v=VGx-TiQHx4Lc.

*Download software and get started!*

- Save and extract the 'Reindeer_counting_drone_imagery.zip' to your computer or hard disk. The folder and metadata require about 4 GB of space so make sure you have enough.

*Set up DotDotGoose software*

- Click and open the dotdotgoose.exe file in the 'Reindeer_counting_drone_imagery' folder
- Click on 'Load' in the bottom left corner. Find the imagery folder "drone_imagery_SAS_2021" and select the point file '**template_reindeer_counting.pnt**'
- In Survey Id at the top left panel: put your first name and last name with underscore e.g. ole_olesen. This will create a column in the metadata with your name.
- Click the Save button and <u>save a point file with your own name</u> (e.g. ole_olesen.pnt) into the same folder as the drone imagery 'drone_imagery_SAS_2021'. It is important that it is the same folder as the imagery if not the save will not work!
- If you need to close the program and finish at another time, you can open your point file in the DotDotGoose software by locating the file and click Import.

**Reindeer detection and assigning objects to categories**

*Time tracking*

- We would like to know how long it takes for each observer to scan through each transect line. The name of each jpeg file starts with the transect number (e.g Line_1, Line_2).
- When you are about to start on the first image of the transect (e.g. Line_1_tile_100.jpeg) write down the time in 'time_start' from the Custom Fields (right side panel) from your computer clock (e.g. 09:54).
- When have scanned all images in the transect (e.g. last image is Line_1_tile_99.jpeg) write down the time in time_stop (e.g. 11:00) on this last image of Line_1.
- Do this for every transect line (Line_1 to Line_6) so we get the start and end time for each transect. Please try to complete every transect line in one go, but if you need to take breaks write down the end time and start time as well so breaks can be subtracted.
- **Remember to save frequently and when you take breaks.**

*Reindeer scanning method*

- For each image, scan the full-scale image quickly from grid to grid with your eyes (see example below). It might be useful to move your mouse as a guide.
- If you can't find an object of interest, go to the next image by pressing **the down arrow key** on your keyboard.
- If you want to go back to any previous images use the **up arrow key** or double click on a specific photo in the Summary table.

- **If you do find an object of interest**, zoom in on it to check if it is a reindeer or carcass by scrolling with your mouse or use the zoom buttons in the right bottom corner (you can also drag the image up, down and sideways by clicking and holding the mouse in).

- To mark a reindeer or carcass, you click on the category you want to assign on the left side panel (see left image below). Hold the Ctrl key in while you click on the object in the image. A dot will be created over the reindeer.
- You can double check that the right category was assigned to the object for that image by looking at the Summary table on the left panel (see right image below).
- NB! If you accidentally make a point or assign wrong category and need to remove it from the image, press and hold the Shift key on your keyboard, then left click and drag the mouse to draw a box around the points you'd like to delete. A red circle around your point will show up. Press the Delete key to remove the point.

*References*

Ersts,P.J.[Internet] DotDotGoose (version 1.5.1). American Museum of Natural History, Center for Bio-diversity and Conservation. Available from https://biodiversityinformat-ics.amnh.org/open_source/dotdotgoose. Accessed on 2021-12-7.

**Appendix C: Detection probability from UAV imagery**

The linear mixed effects models were developed based on two sources of detection errors in mind. The probability that 1) an observer detects a reindeer on an image (presence/absence model) and 2) when they do, how many reindeer are detected on that image (counts model). The reason for this was also to develop detection models that would fit the two-function process in the density model. For the presence/absence model, all reindeer detected by observers (verified as a reindeer (1) or not (0) by authors) were given an ID based on their GPS coordinates. The image covariates median luminance, mean red, mean green, and mean blue channels were extracted from each image using the package imageR. The RGB greenness index (G-B, [61]) was calculated to identify green background (low values = dark green, high values = light green). High values in the red and blue channel indicated grey, gravely backgrounds. The models used glmer() in the lme4 package in R. Due to multicollinearity issues, it was decided to put each covariate with observer as a random effect in separate glmer models.

Presence/absence model

- Binomial GLMER
- 5 separate models with observer id as a random effect and each of the fixed effects median luminance, mean red, green, and blue channels per image. We only show the predicted effect plots for the fixed effects with a statistical significance (p>0.05) below (intercepts and standard error in results section).
- Response variable: reindeer seen (1) or reindeer not seen (0) by observers
- Sample size n=234
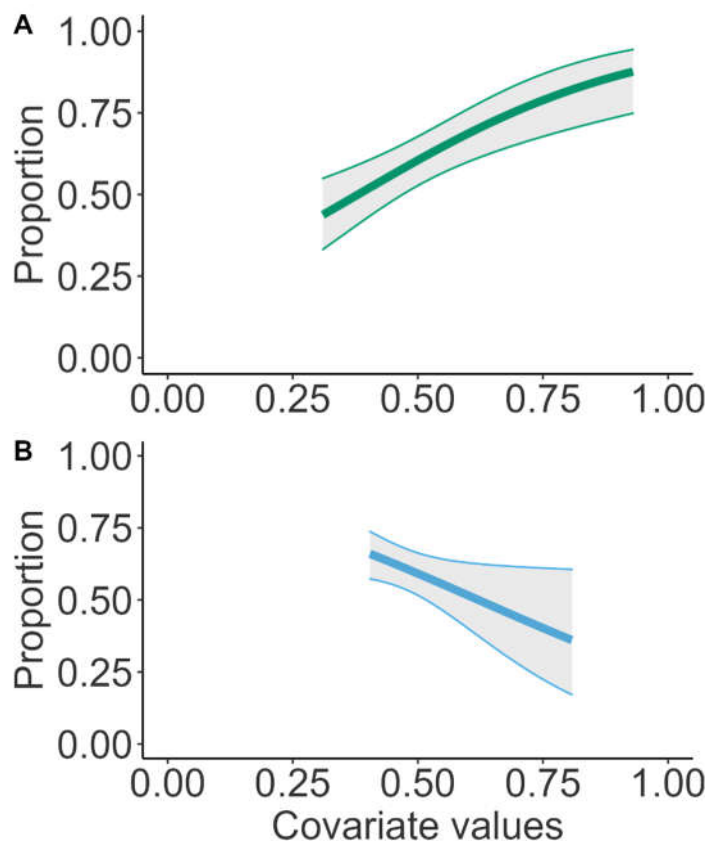
**Figure C1.** Predicted effects of covariates with p>0.01 in the GLMER presence/absence model. A) Predicted effects of the greenness index, B) predicted effects of the mean blue channel.

Counts model

- Poisson GLMER.
- Five models with observer id as a random effect and each of the fixed effects median luminance, mean red, green, and blue channels per image (intercepts and standard error in results section).
- Response variable: number of reindeer seen on image per observer
- Sample size n=179
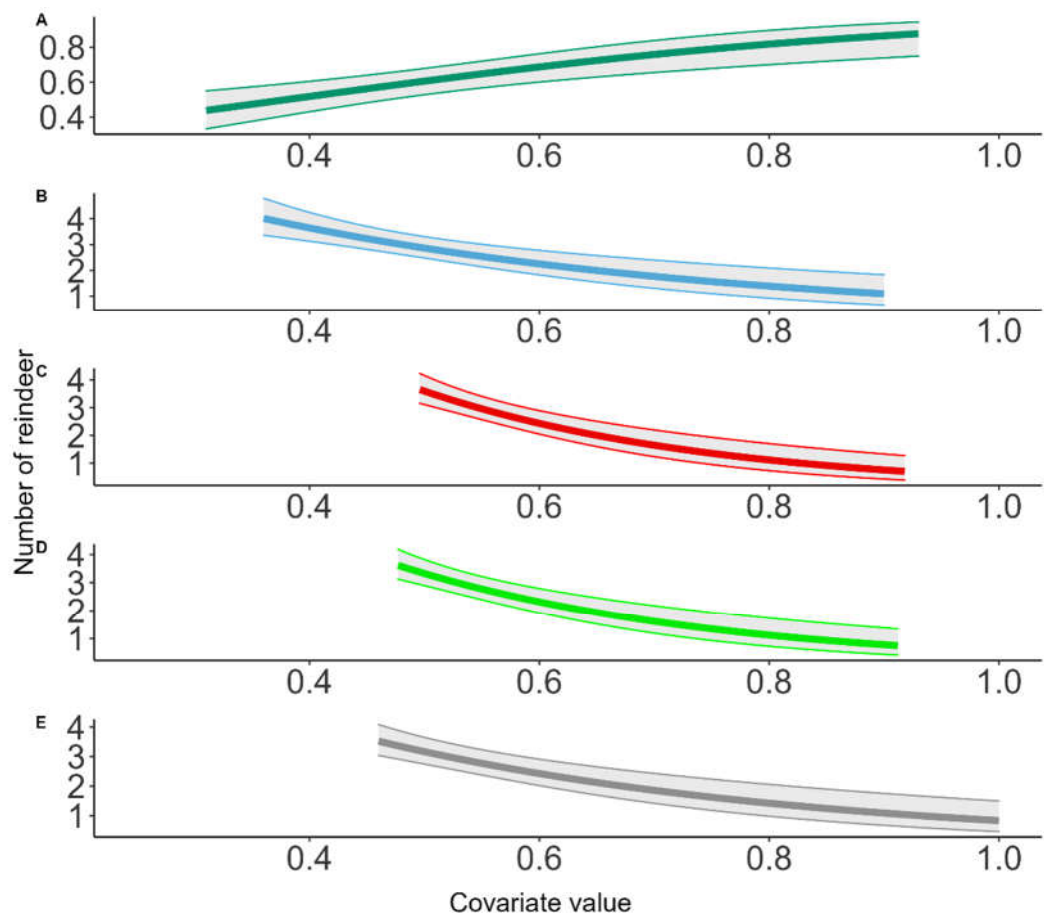
**Figure C2**. Predicted effects of each covariate in the five separate GLMER counts model. A) greenness index, B) mean blue channel, C) mean red channel, D) mean green channel, E) median luminance.

**Appendix D: UAV density model for estimating reindeer abundance with Hurdle density model**

**Table D1.** UAV density model obtained from UAV sampling in Sassendalen in 2021. We used the most parsimonious density model from Le Moullec *et al*. [42], which modelled individuals per segment as a function of NDVI using a hurdle density model with a zero-truncated negative binomial distribution with a dispersion parameter. This model was fitted using the restricted maximum likelihood (REML) framework.

| | | **Hurdle density model Adventdalen** | |
|---|---|---|---|
| | | $\beta \pm SE$ | P |
| Count model | Intercept | -2.61 ± 82.8 | 0.975 |
| | NDVI* | -9.59 ± 7.15 | 0.180 |
| P/A model | Intercept | -7.00 ± 1.40 | <0.05 |
| | NDVI | 6.67 ± 2.15 | **0.002** |

**Appendix E: Total counts from the long-term monitoring in Adventdalen – background data and results**

**Field methods**

The annual total population count of reindeer in Adventdalen was conducted in summer (28 June to 4 July 2019) after calving. During the count, reindeer were categorized by age as calves, yearlings, or adults (≥2 yr. old) based on body size and antler characteristics. The geographic position of individual reindeer or groups were noted. Four to six observers walked separate, predefined routes scanning the entire area with 10 × 42 mm binoculars. At this time of the year, reindeer still have parts of their winter fur, making them conspicuous against the open tundra landscape. Because of the open landscape and the stationary behavior of reindeer, counts are assumed to be close to the actual population number in summer after calving (see Le Moullec et al. [20]).

**Statistical analyses**

The values of all average maxNDVI pixels (240 x240 m) in the sampling area (Adventdalen below 250 metres) was extracted (N=3262 pixels), including all pixels with at least one geographic position of a reindeer observation (n=437 pixels, min positions per pixel=1, max positions per pixel = 22). 1527 reindeer groups had positional information (out of 1668 reindeer groups). Mean reindeer group size was 3.2 reindeer. The hurdle logit model was applied to this dataset with NDVI as a covariate and observations per pixel as a response variable. The best model was determined by AIC. Based on the best model from the total counts, a density map was created across the Sassendalen valley in the same area as the helicopter surveyed area.
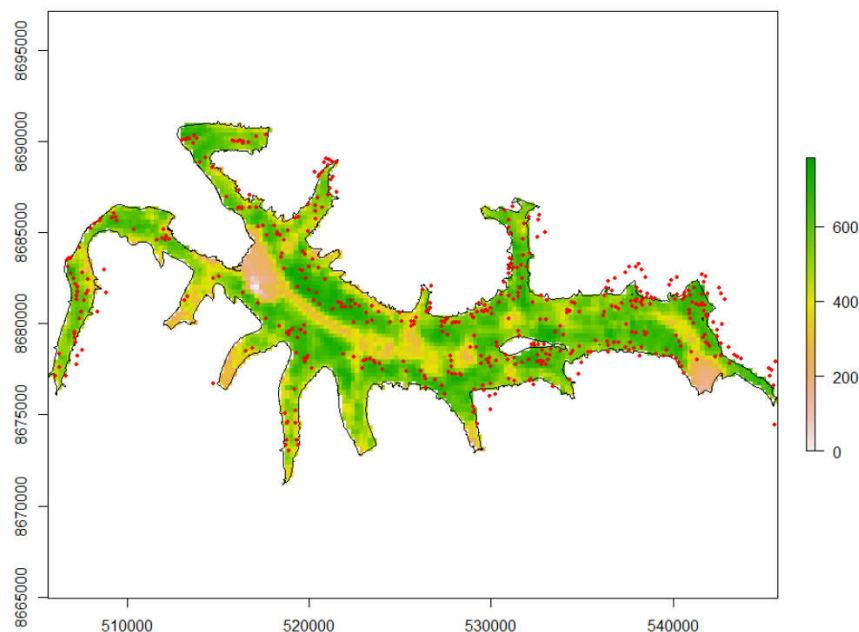
**Figure E1.** Reindeer geographic positions in the neighbouring valley Adventdalen (N=1527).

**Table E1.** Independent total counts density model obtained from ground counts in a neighboring valley. We used the most parsimonious density total counts model from Le Moullec *et al.* [42], which modelled individuals per segment as a function of NDVI using a hurdle density model with a zero-truncated negative binomial distribution with a dispersion parameter. This model was fitted using the restricted maximum likelihood (REML) framework.

| | | **Hurdle density model Adventdalen** | |
|---|---|---|---|
| | | $\beta \pm SE$ | P |
| Count model | Intercept | -1.04 ± 0.57 | 0.07* |
| | NDVI* | 0.003 ± 0.0009 | 0.002 |
| P/A model | Intercept | -4.59 ± 0.33 | <0.05 |
| | NDVI | 0.004 ± 0.0005 | 0.02 |

# References

1. Nichols, J.D.; Williams, B.K. Monitoring for conservation. *Trends in Ecology & Evolution* **2006**, *21*, 668-673.

2. Williams, B.K.; Nichols, J.D.; Conory, M.J. Analysis and Management of Wildlife Populations. *Academic Press, San Diego, California, USA.* **2002**.

3. Forsyth, D.M.; Comte, S.; Davis, N.E.; Bengsen, A.J.; Cote, S.D.; Hewitt, D.G.; Morellet, N.; Mysterud, A. Methodology matters when estimating deer abundance: a global systematic review and recommendations for improvements. *Journal of Wildlife Management* **2022**, *86*, doi:10.1002/jwmg.22207.

4. Thompson, W.L.; White, G.C.; Gowan, C. Chapter 3 - Enumeration Methods. In *Monitoring Vertebrate Populations*, Thompson, W.L., White, G.C., Gowan, C., Eds.; Academic Press: San Diego, 1998; pp. 75-121.

5. Marlène Gamelon; Josh A. Firth; Mathilde Le Moullec; William K. Petry; Salguero-Gòmez, R. Longitudinal demographic data collection. In *Demographic Methods across the Tree of Life*, Roberto Salguero-Gomez, M.G., Ed.; Oxford Academic: Oxford, 2021.

6. ENETWILD consortium; Grignolio, S.; Apollonio, M.; Brivio, F.; Vicente, J.; Acevedo, P.; P., P.; Petrovic, K.; Keuling, O. Guidance on estimation of abundance and density data of wild ruminant population: methods, challenges, possibilities. **2020**, *17*, 1876E, doi:https://doi.org/10.2903/sp.efsa.2020.EN-1876.

7. Wang, D.L.; Shao, Q.Q.; Yue, H.Y. Surveying Wild Animals from Satellites, Manned Aircraft and Unmanned Aerial Systems (UASs): A Review. *Remote Sens.* **2019**, *11*, doi:10.3390/rs11111308.

8. Pereira, J.A.; Varela, D.; Scarpa, L.J.; Frutos, A.E.; Fracassi, N.G.; Lartigau, B.V.; Pina, C.I. Unmanned aerial vehicle surveys reveal unexpectedly high density of a threatened deer in a plantation forestry landscape. *Oryx* **2022**, doi:10.1017/s0030605321001058.

9. Schofield, G.; Esteban, N.; Katselidis, K.A.; Hays, G.C. Drones for research on sea turtles and other marine vertebrates - A review. *Biological Conservation* **2019**, *238*, doi:10.1016/j.biocon.2019.108214.

10. Fettermann, T.; Fiori, L.; Gillman, L.; Stockin, K.A.; Bollard, B. Drone Surveys Are More Accurate Than Boat-Based Surveys of Bottlenose Dolphins (Tursiops truncatus). **2022**, *6*, 82.

11. Hodgson, J.C.; Mott, R.; Baylis, S.M.; Pham, T.T.; Wotherspoon, S.; Kilpatrick, A.D.; Raja Segaran, R.; Reid, I.; Terauds, A.; Koh, L.P. Drones count wildlife more accurately and precisely than humans. **2018**, *9*, 1160-1167, doi:https://doi.org/10.1111/2041-210X.12974.

12. Forsyth, D.M.; MacKenzie, D.I.; Wright, E.F. Monitoring ungulates in steep non-forest habitat: a comparison of faecal pellet and helicopter counts. *New Zealand Journal of Zoology* **2014**, *41*, 248-262, doi:10.1080/03014223.2014.936881.

13. Noyes, J.H.; Johnson, B.K.; Riggs, R.A.; Schlegel, M.W.; Coggins, V.L. Assessing aerial survey methods to estimate elk populations: a case study. *Wildlife Society Bulletin* **2000**, *28*, 636-642.

14. Poole, K.G.; Cuyler, C.; Nymand, J. Evaluation of caribou Rangifer tarandus groenlandicus survey methodology in West Greenland. *Wildlife Biology* **2013**, *19*, 225-239, doi:10.2981/12-004.

15. Davis, K.L.; Silverman, E.D.; Sussman, A.L.; Wilson, R.R.; Zipkin, E.F. Errors in aerial survey count data: Identifying pitfalls and solutions. *Ecology and Evolution* **2022**, *12*, doi:10.1002/ece3.8733.

16. Reilly, B.K.; van Hensbergen, H.J.; Eiselen, R.J.; Fleming, P.J.S. Statistical power of replicated helicopter surveys in southern African conservation areas. *African Journal of Ecology* **2017**, *55*, 198-210, doi:10.1111/aje.12341.

17. Dyal, J.; Miller, K.V.; Cherry, M.J.; D'Angelo, G.J. Estimating Sightability for Helicopter Surveys Using Surrogates of White-Tailed Deer. *Journal of Wildlife Management* **2021**, *85*, 887-896, doi:10.1002/jwmg.22040.

18. Mansson, J.; Hauser, C.E.; Andren, H.; Possingham, H.P. Survey method choice for wildlife management: the case of moose Alces alces in Sweden. *Wildlife Biology* **2011**, *17*, 176-190, doi:10.2981/10-052.

19. Gentle, M.; Finch, N.; Speed, J.; Pople, A. A comparison of unmanned aerial vehicles (drones) and manned helicopters for monitoring macropod populations %J Wildlife Research. **2018**, *45*, 586-594, doi:https://doi.org/10.1071/WR18034.

20. Le Moullec, M.; Pedersen, A.O.; Yoccoz, N.G.; Aanes, R.; Tufto, J.; Hansen, B.B. Ungulate population monitoring in an open tundra landscape: distance sampling versus total counts. *Wildlife Biology* **2017**, doi:10.2981/wlb.00299.

21. Delplanque, A.; Foucher, S.; Lejeune, P.; Linchant, J.; Théau, J. Multispecies detection and identification of African mammals in aerial imagery using convolutional neural networks. **2022**, *8*, 166-179, doi:https://doi.org/10.1002/rse2.234.

22. Yang, F.; Shao, Q.; Jiang, Z. A Population Census of Large Herbivores Based on UAV and Its Effects on Grazing Pressure in the Yellow-River-Source National Park, China. *International journal of environmental research and public health* **2019**, *16*, doi:10.3390/ijerph16224402.

23. Butcher, P.A.; Colefax, A.P.; Gorkin, R.A.; Kajiura, S.M.; López, N.A.; Mourier, J.; Purcell, C.R.; Skomal, G.B.; Tucker, J.P.; Walsh, A.J.; et al. The Drone Revolution of Shark Science: A Review. **2021**, *5*, 8.

24. Buckland, S.T.; Anderson, D.R.; Burnham, K.P.; Laake, J.L.; Borchers, D.L.; Thomas, L. Introduction to Distance Sampling. Estimating abundance of biological populations. . *Oxford University Press* **2001**, 432.

25. Linnell, J.D.C.; Cretois, B.; Nilsen, E.B.; Rolandsen, C.M.; Solberg, E.J.; Veiberg, V.; Kaczensky, P.; Van Moorter, B.; Panzacchi, M.; Rauset, G.R.; et al. The challenges and opportunities of coexisting with wild ungulates in the human-dominated landscapes of Europe's Anthropocene. *Biological Conservation* **2020**, *244*, doi:10.1016/j.biocon.2020.108500.

26. Solberg, E.J.; Sæther, B.E. Hunter observations of moose Alces alces as a management tool. *Wildlife Biology* **1999**, *5*, 107-117.

27. Pfeffer, S.E.; Spitzer, R.; Allen, A.M.; Hofmeester, T.R.; Ericsson, G.; Widemo, F.; Singh, N.J.; Cromsigt, J. Pictures or pellets? Comparing camera trapping and dung counts as methods for estimating population densities of ungulates. *Remote Sensing in Ecology and Conservation* **2018**, *4*, 173-183, doi:10.1002/rse2.67.

28. Pal, R.; Bhattacharya, T.; Qureshi, Q.; Buckland, S.T.; Sathyakumar, S. Using distance sampling with camera traps to estimate the density of group-living and solitary mountain ungulates. *Oryx* **2021**, *55*, 668-676, doi:10.1017/s003060532000071x.

29. Schroeder, N.M.; Panebianco, A.; Musso, R.G.; Carmanchahi, P. An experimental approach to evaluate the potential of drones in terrestrial mammal research: a gregarious ungulate as a study model. *Royal Society Open Science* **2020**, *7*, doi:10.1098/rsos.191482.

30. Witczuk, J.; Pagacz, S.; Zmarz, A.; Cypel, M. Exploring the feasibility of unmanned aerial vehicles and thermal imaging for ungulate surveys in forests - preliminary results. *International Journal of Remote Sensing* **2018**, *39*, 5504-5521, doi:10.1080/01431161.2017.1390621.

31. Beaver, J.T.; Baldwin, R.W.; Messinger, M.; Newbolt, C.H.; Ditchkoff, S.S.; Silman, M.R. Evaluating the Use of Drones Equipped with Thermal Sensors as an Effective Method for Estimating Wildlife. *Wildlife Society Bulletin* **2020**, *44*, 434-443, doi:10.1002/wsb.1090.

32. Torney, C.J.; Lamont, M.; Debell, L.; Angohiatok, R.J.; Leclerc, L.M.; Berdahl, A.M. Inferring the rules of social interaction in migrating caribou. *Philosophical Transactions of the Royal Society B-Biological Sciences* **2018**, *373*, doi:10.1098/rstb.2017.0385.

33. Graves, T.A.; Yarnall, M.J.; Johnston, A.N.; Preston, T.M.; Chong, G.W.; Cole, E.K.; Janousek, W.M.; Cross, P.C. Eyes on the herd: Quantifying ungulate density from satellite, unmanned aerial systems, and GPScollar data. *Ecological Applications* **2022**, doi:10.1002/eap.2600.

34. Descamps, S.; Aars, J.; Fuglei, E.; Kovacs, K.M.; Lydersen, C.; Pavlova, O.; Pedersen, A.O.; Ravolainen, V.; Strom, H. Climate change impacts on wildlife in a High Arctic archipelago - Svalbard, Norway. *Global Change Biology* **2017**, *23*, 490-502, doi:10.1111/gcb.13381.

35. van der Wal, R.; Bardgett, R.D.; Harrison, K.A.; Stien, A. Vertebrate herbivores and ecosystem control: cascading effects of faeces on tundra ecosystems. *Ecography* **2004**, *27*, 242-252, doi:10.1111/j.0906-7590.2004.03688.x.

36. Peeters, B.; Pedersen, Å.Ø.; Veiberg, V.; Hansen, B.B. Hunting quotas, selectivity and stochastic population dynamics challenge the management of wild reindeer. *Climate Research* **2021**, doi:10.3354/cr01668.

37. Hansen, B.B.; Gamelon, M.; Albon, S.D.; Lee, A.M.; Stien, A.; Irvine, R.J.; Saether, B.E.; Loe, L.E.; Ropstad, E.; Veiberg, V.; et al. More frequent extreme climate events stabilize reindeer population dynamics. *Nature Communications* **2019**, *10*, doi:10.1038/s41467-019-09332-5.

38. Loe, L.E.; Liston, G.E.; Pigeon, G.; Barker, K.; Horvitz, N.; Stien, A.; Forchhammer, M.; Getz, W.M.; Irvine, R.J.; Lee, A.; et al. The neglected season: Warmer autumns counteract harsher winters and promote population growth in Arctic reindeer. *Global Change Biology* **2021**, *27*, 993-1002, doi:https://doi.org/10.1111/gcb.15458.

39. Solberg, E.J.; STrand, O.; Veiberg, V.; Andersen, R.; Heim, M.; Rolandsen, C.M.; Langvatn, R.; Holmstrøm, F.; Solem, M.I.; Eriksen, R.; et al. Hjortevilt 1991-2011. Oppsummeringsrapport fra Overvåkingsprogrammet for hjortevilt. *NINA rapport 885* **2012**.

40. Governor of Svalbard. Plan for forvaltning av svalbardrein, kunnskaps- og forvaltningsstatus. *Rapport 1/2009*. **2009**.

41. Albon, S.D.; Irvine, R.J.; Halvorsen, O.; Langvatn, R.; Loe, L.E.; Ropstad, E.; Veiberg, V.; Van Der Wal, R.; Bjørkvoll, E.M.; Duff, E.I.; et al. Contrasting effects of summer and winter warming on body mass explain population dynamics in a food-limited Arctic herbivore. *Global Change Biology* **2017**, *23*, 1374-1389, doi:10.1111/gcb.13435.

42. Le Moullec, M.; Pedersen, Å.Ø.; Stien, A.; Rosvold, J.; Hansen, B.B. A century of conservation: The ongoing recovery of svalbard reindeer. *Journal of Wildlife Management* **2019**, *83*, 1676-1686, doi:10.1002/jwmg.21761.

43. Ims, R.A.; Jepsen, J.U.; Stien, A.; Yoccoz, N.G. *Science Plan for COAT: Climate-ecological Observatory for Arctic Tundra*; Fram Centre: Tromsø, 2013.

44. Hann, R.; Altstädter, B.; Betlem, P.; Deja, K.; Dragańska-Deja, K.; Ewertowski, M.; Hartvich, F.; Jonassen, M.; Lampert, A.; Laska, M.; et al. Scientific Applications of Unmanned Vehicles in Svalbard. *SESS report 2020, Svalbard Integrated Arctic Earth Observing System* **2021**, doi:https://doi.org/10.5281/zenodo.4293283.

45. Eischeid, I.; Soininen, E.M.; Assmann, J.J.; Ims, R.A.; Madsen, J.; Pedersen, Å.Ø.; Pirotti, F.; Yoccoz, N.G.; Ravolainen, V.T. Disturbance Mapping in Arctic Tundra Improved by a Planning Workflow for Drone Studies: Advancing Tools for Future Ecosystem Monitoring. **2021**, *13*, 4466.

46. Johansen, B.E.; Karlsen, S.R.; Tommervik, H. Vegetation mapping of Svalbard utilising Landsat TM/ETM plus data. *Polar Rec.* **2012**, *48*, 47-63, doi:10.1017/s0032247411000647.

47. Elvebakk, A. A vegetation map of Svalbard on the scale 1 : 3.5 mill. *Phytocoenologia* **2005**, *35*, 951-967, doi:10.1127/0340-269x/2005/0035-0951.

48. Elvebakk, A. Bioclimatic delimitation and subdivision of the Arctic. *Norske Videnskaps-Akademi* **1999**, *In: Nordal, I., and V.Y. Razzhivin (editors). The species concept in the high north – A panarctic flora initiative.*, 81–112.

49. Derocher, A.E.; Wiig, O.; Bangjord, G. Predation of Svalbard reindeer by polar bears. *Polar Biol.* **2000**, *23*, 675-678, doi:10.1007/s003000000138.

50. Stempniewicz, L.; Kulaszewicz, I.; Aars, J. Yes, they can: polar bears Ursus maritimus successfully hunt Svalbard reindeer Rangifer tarandus platyrhynchus. *Polar Biol.* **2021**, 2199–2206, doi:10.1007/s00300-021-02954-w.

51. Solberg, E.J.; Jordhøy, P.; Strand, O.; Aanes, R.; Loison, A.; Sæther, B.E.; Linnell, J.D.C. Effects of density-dependence and climate on the dynamics of a Svalbard reindeer population. *Ecography* **2001**, *24*, 441-451.

52. Stien, A.; Ims, R.A.; Albon, S.D.; Fuglei, E.; Irvine, R.J.; Ropstad, E.; Halvorsen, O.; Loe, L.E.; Veiberg, V.; Yoccoz, N.G. Congruent responses to weather variability in high arctic herbivores. *Biology Letters* **2012**, *8*, 1002-1005.

53. Hansen, B.B.; Grøtan, V.; Aanes, R.; Sæther, B.-E.; Stien, A.; Fuglei, E.; Ims, R.A.; Yoccoz, N.G.; Pedersen, Å.Ø.J.S. Climate events synchronize the dynamics of a resident vertebrate community in the high Arctic. **2013**, *339*, 313-315.

54. Marques, T.A.; Buckland, S.T.; Bispo, R.; Howland, B. Accounting for animal density gradients using independent information in distance sampling surveys. *Statistical Methods and Applications* **2013**, *22*, 67-80, doi:10.1007/s10260-012-0223-2.

55. Pedersen, Å.Ø.; Bårdsen, B.J.; Veiberg, V.; Hansen, B.B. Jegernes egne data. Analyser av jaktstatistikk og kjevemateriale fra svalbardrein. *Norsk Polarinstitutt Kortrapport 27* **2014**.

56. Peeters, B.; Pedersen2, Å.Ø.; Veiberg, V.; Hansen, B.B. Hunting quotas, selectivity and stochastic population dynamics challenge the management of wild reindeer. *Climate Research* **2021**, doi:10.3354/cr01668.

57. Karlsen, S.R.; Elvebakk, A.; Hogda, K.A.; Grydeland, T. Spatial and Temporal Variability in the Onset of the Growing Season on Svalbard, Arctic Norway - Measured by MODIS-NDVI Satellite Data. *Remote Sensing* **2014**, *6*, 8088-8106, doi:10.3390/rs6098088.

58. Karlsen, S.R.; Anderson, H.B.; van der Wal, R.; Hansen, B.B. A new NDVI measure that overcomes data sparsity in cloud-covered regions predicts annual variation in ground-based estimates of high arctic plant productivity. *Environ. Res. Lett.* **2018**, *13*, 12, doi:10.1088/1748-9326/aa9f75.

59. R Core Team. R: A language and environment for statistical computing. R Foundation for Sta-tistical Computing, Vienna, Austria. URL https://www.R-project.org/. **2021**.

60. Miller, D.L.; Burt, M.L.; Rexstad, E.A.; Thomas, L.J.M.i.E.; Evolution. Spatial models for distance sampling data: recent developments and future directions. **2013**, *4*, 1001-1010.

61. Kawashima, S.; Nakatani, M. An Algorithm for Estimating Chlorophyll Content in Leaves Using a Video Camera. *Annals of Botany* **1998**, *81*, 49-54, doi:10.1006/anbo.1997.0544 %J Annals of Botany.

62. Sun, C.; Beirne, C.; Burgar, J.M.; Howey, T.; Fisher, J.T.; Burton, A.C. Simultaneous monitoring of vegetation dynamics and wildlife activity with camera traps to assess habitat change. **2021**, *7*, 666-684, doi:https://doi.org/10.1002/rse2.222.

63. Jeliazkov, A.; Gavish, Y.; Marsh, C.J.; Geschke, J.; Brummitt, N.; Rocchini, D.; Haase, P.; Kunin, W.E.; Henle, K. Sampling and modelling rare species: Conceptual guidelines for the neglected majority. **2022**, *28*, 3754-3777, doi:https://doi.org/10.1111/gcb.16114.

64. Dujon, A.M.; Ierodiaconou, D.; Geeson, J.J.; Arnould, J.P.Y.; Allan, B.M.; Katselidis, K.A.; Schofield, G. Machine learning to detect marine animals in UAV imagery: effect of morphology, spacing, behaviour and habitat. **2021**, *7*, 341-354, doi:https://doi.org/10.1002/rse2.205.